In summary, the temperature effect on the arrangement of stilbenoid dendrimers on HOPG is presented in this work. It is seen that **SD12** molecules form well-ordered hexagonal nanostructures at 16 °C. However, if the adlayer is annealed at 65 °C, the adlayer structure is changed into a well-ordered parallelogram nanostructure in a close-packed arrangement with a higher surface coverage. The phenomenon described here supports the earlier reports on two liquid-crystalline phases for **SD12**.[15] The results in this research are useful in understanding the phase transition of **SD12** as well as metastable complex systems with temperature.

Experimental Section

Synthetic methods: **SD12**, **SD14**, and **SD16** were prepared as described in the literature.[15]

Sample preparation for STM observation: The molecules were dissolved in toluene (HPLC grade, Aldrich) with a concentration of less than 0.01 mg mL^{-1}. The self-assembled adlayers were prepared by depositing a droplet of this solution onto a freshly cleaved surface of HOPG (quality ZYB, Digital Instruments). The STM images in Figure 1 a, 2 a and 3 were acquired after the solvent evaporated at 16 °C; the STM images of Figure 1 b and Figure 2 c after the substrate was kept at 65 °C for about 2 h and slowly cooled down to room temperature. The experiment was performed with a Nanoscope IIIa SPM (Digital Instruments, Santa Barbara, CA) under ambient conditions. STM tips were mechanically formed Pt/Ir wires (90/10). All STM images were recorded using the constant current mode. The specific tunneling conditions are given in the figure captions. The preliminary simulations were performed using the Hyperchem software to model the structures of the molecules.

The authors thank the National Natural Science Foundation (Grant Nos. 20103008; 20073053; 20121301) and the Foundation from Chinese Academy of Sciences for financial support. Support from the National Key Project on Basic Research (grant G2000077501) is also acknowledged.

[1] J. Frommer, *Angew. Chem.* **1992**, *104*, 1325; *Angew. Chem. Int. Ed. Engl.* **1992**, *31*, 1298.
[2] S. D. Feyter, P. C. M. Grim, M. Rücher, P. Vanoppen, C. Meiners, M. Sieffert, S. Valiyaveettil, K. Müllen, F. C. De Schryver, *Angew. Chem.* **1998**, *110*, 1281; *Angew. Chem. Int. Ed.* **1998**, *37*, 1223.
[3] T. A. Jung, R. R.Schlittler, J. K. Gimzewski, *Nature* **1997**, *386*, 696.
[4] M. de Wild, S. Berner, H. Suzuki, H. Yanagi, D. Schlettwein, S. Ivan, A.Baratoff, H.-J. Guentherodt, T. A. Jung, *ChemPhysChem* **2002**,*3*, 825.
[5] M. Böhringer, K. Morgenstern, W.-D. Schneider, R. Berndt, *Angew. Chem.* **1999**, *111*, 832; *Angew. Chem. Int. Ed.* **1999**, *38*, 821.
[6] A. Haran, D. H. Waldeck, R. Naaman, E. Moons, D. Cahen, *Science* **1994**, *263*, 948.
[7] H. B. Fang, L. C. Giancarlo, G. W. Flynn, *J. Phys. Chem. B* **1999**, *103*, 5712.
[8] a) J. V. Barth, J. Weckesser, C. Cai, P. Günter, L. Bürgi, O. Jeandupeux, K. Kern, *Angew. Chem.* **2000**, *112*, 1285; *Angew. Chem. Int. Ed.* **2000**, *39*, 1230; b) J. Weckesser, A. De Vita, J. V. Barth, C. Cai, K. Kern, *Phys. Rev. Lett.* **2001**, *87*, 096101 – 1.
[9] P. Wu, Q. D. Zeng, S. D. Xu, C. Wang, S. X. Yin, C. L. Bai, *ChemPhysChem* **2001**, *12*, 750.
[10] T. Yokoyama, S. Yokoyama, T. Kamikado, Y. Okuno, S. Mashiko, *Nature* **2001**, *413*, 619.
[11] R. Yamada, H. Wano, K. Uosaki, *Langmuir* **2000**, *16*, 5523.
[12] P. Samorf, A. Fechtenkötter, F. Jäckel, T. Böhme, K. Müllen, J. P. Rabe, *J. Am. Chem. Soc.* **2001**, *123*, 11 462.
[13] H. B. Yu, C. S. Jiang, P. Ebert, X. D. Wang, J. M. White, Q. Niu, Z. Zhang, C. K. Shih, *Phys. Rev. Lett.* **2002**, *88*, 016102 – 1.
[14] H. Meier, *Angew. Chem.* **1992**, *104*, 1425; *Angew. Chem. Int. Ed. Engl.* **1992**, *31*, 1399.
[15] H. Meier, M. Lehmann, *Angew. Chem.* **1998**, *110*, 666; *Angew. Chem. Int. Ed.* **1998**, *37*, 643.
[16] a) X. H. Qiu, C. Wang, Q. D. Zeng, B. Xu, S. X. Yin, H. N. Wang, S. D. Xu, C. L. Bai, *J. Am. Chem. Soc.* **2000**, *122*, 5550; b) C. J. Li, Q. D. Zeng, P. Wu, S. L. Xu, C. Wang, Y. H. Qiao, L. J. Wan, C. L. Bai, *J. Phys. Chem. B* **2002**, *106*, 13 262.
[17] F. Charra, J. Cousty, *Phys. Rev. Lett.* **1998**, *80*, 1682.
[18] V. S. Lyer, K. Yoshimura, V. Enkelmann, R. Epsch, J. P. Rabe, K. Müllen, *Angew. Chem.* **1998**, *110*, 2843; *Angew. Chem. Int. Ed.* **1998**, *37*, 2696.
[19] K. Eichhorst-Gerner, A. Stable, G. Moessner, D. Declerq, S. Valigaveettil, V. Enkelmann, K. Müllen, J. P. Rabe, *Angew. Chem.* **1996**, *108*, 1599; *Angew. Chem. Int. Ed. Engl.* **1996**, *35*, 1492.
[20] R. Hentschke, B. L. Schurmann, J. P. Rabe, *J. Chem. Phys.* **1992**, *96*, 6213.
[21] a) J. V. Barth, *Surf. Sci. Rep.* **2000**, *40*, 75; b) T. Ala-Nissila, R. Ferrando, S. C. Ying, *Adv. Phys.* **2002**, *51*, 949.

Received: August 23, 2002 [Z492]
Revised: May 20, 2003

Determination of the Electron Lifetime in Nanocrystalline Dye Solar Cells by Open-Circuit Voltage Decay Measurements

Arie Zaban,*[a] Miri Greenshtein,[a] and Juan Bisquert*[b]

KEYWORDS:
charge transfer · nanostructures · semiconductors · solar cells

Recently, a new class of photoelectrochemical cells based on nanoscaled porous metal oxide semiconductors (dye-sensitized solar cell) has promoted intense research due to the prospects of cheap and efficient conversion of visible light into electricity and of new applications such as transparent solar cells.[1] It is widely agreed that the electron-transfer kinetics play a major role in determining the energy conversion efficiency of dye-sensitized solar cells.[2, 3] Herein, we develop a new powerful tool to study the electron lifetime in dye solar cells as a function of the photovoltage (V_{oc}); the open-circuit voltage-decay (OCVD) technique. This technique has certain advantages over frequen-

[a] *Prof. A. Zaban, M. Greenshtein*
Department of Chemistry
Bar-Ilan University
Ramat-Gan 52900 (Israel)
E-mail: zabana@mail.biu.ac.il
[b] *Dr. J. Bisquert*
Departament de Ciències Experimentals
Universitat Jaume I, 12080 Castelló (Spain)
E-mail: bisquert@uji.es

 DOI: 10.1002/cphc.200200615

cy or steady-state-based methods: a) it provides a continuous reading of the lifetime as a function of V_{oc} at high-voltage resolution, b) it is experimentally much simpler, and c) the data treatment is outstandingly simple (basically, it consists of two derivatives) for obtaining the main quantities that provide information on the recombination mechanisms.

In order to treat such data and analyse the information contained in it, we present a new theoretical framework that derives the electron lifetime from a general recombination rate, ($U(n)$), which incorporates the possible complex-recombination mechanisms in dye solar cells, such as a higher reaction order electrontransfer mediated by trapping and detrapping. These mechanisms will be conveniently represented by an effective recombination order (β) that governs the change of the lifetime over a broad variation of internal conditions in the solar cell. We also provide a procedure to extract the fundamental information on the electron lifetime from the measured OCVD curves. We will show the equivalence, in broad terms, with the lifetime, measured by intensity-modulated photovoltage spectroscopy (IMVS) as well as the unique observations revealed by the high-voltage resolution.

Dye-sensitised solar cells consist of a dyed nanoporous semiconductor photoelectrode permeated with a redox electrolyte. When the cell is illuminated at open circuit, the free electron density in the semiconductor nanostructure (n) is affected by two main processes. 1) Electron photogeneration, which is achieved by electron injection from the photoexcited dye molecules attached to the semiconductor nanoparticle surface into the semiconductor conduction band (cb), that is, photo-oxidation of the dye molecules. This photogeneration process can be maintained at a stationary rate, because the reduced electrolyte species (electron donors) are able to regenerate the oxidized dye molecules. 2) Recombination of the photogenerated electrons by reaction with electrolyte-oxidised species (which is thought to be predominant in comparison with electron capture by the oxidised dye). Therefore, n increases by photogeneration at a rate $G = \alpha_{abs} I_0$, where I_0 is the incident light intensity, α_{abs} is the absorption coefficient of dye molecules and homogeneous photoinjection is assumed, and decreases by recombination at a rate $U(n)$ that depends on the electron density in the electrode. The overall balance can be expressed by the kinetic Equation (1).

$$\frac{dn}{dt} = -U(n) + \alpha_{abs} I_0 \quad (1)$$

Under constant illumination, the solar cell reaches a photostationary situation in which the free electron density satisfies $U(n) = \alpha_{abs} I_0$. Under these conditions, V_{oc} corresponds to the increase of the quasi-Fermi level of the semiconductor (E_{Fn}) with respect to the dark value (E_{F0}), which equals the electrolyte redox energy ($E_{F0} = E_{redox}$). Therefore, it can be written as Equation (2):[2]

$$V_{oc} = \frac{E_{Fn} - E_{F0}}{e} = \frac{k_B T}{e} \ln\left(\frac{n}{n_0}\right) \quad (2)$$

Here, $k_B T$ is the thermal energy, e is the positive elementary charge, and n_0 is the concentration in the dark. Clearly, the recombination rate has a major impact on the open-circuit voltage obtained at any light intensity.

Information on the properties of the recombination process can be obtained from the correlation $V_{oc}(I_0)$ in the steady state. A much more sensitive method is to determine the characteristic time of recovery when the system is displaced from a steady state at open circuit, that is, the electron lifetime (τ_n). In the dye-solar-cell area, the dominant dynamic technique of this kind is IMVS, which measures the photovoltage in response to a small periodic modulation of the light intensity over a background steady state.[4, 5]

Another way to probe the kinetics of recombination is to monitor the transient of V_{oc} during the relaxation from the illuminated quasiequilibrium state to the dark equilibrium. Although this method is fairly obvious, as far as we know, it has not been fully developed for the study of dye solar cells. A possible reason for this is the huge variation of the photophysical magnitudes in this system when the steady state is varied. Indeed, the results of IMVS showed that the electron lifetime changes exponentially over orders of magnitude when the steady state varies from $V_{oc} = 0$ V to the upper limit, which is ≈ 0.8 V.[4, 5] Therefore, large perturbation techniques involving vast changes of the parameters will, in principle, be much more difficult to interpret than those techniques that function by a small perturbation over a steady state, such as IMVS. However, in the following we show that it is indeed possible to obtain the (variable) electron lifetime from large amplitude OCVD technique. This is facilitated by the fact that in the OCVD the system is kept at open circuit during the transient, and because the internal gradients of carriers are usually low, the measurement of $V_{oc}(t)$ very nearly records a succession of steady states.

The starting point for the V_{oc} decay measurement is the nonequilibrium steady state of a cell illuminated at constant intensity I_0. The illumination is interrupted, and $V_{oc}(t)$ is recorded, while the cell is kept at open circuit. During the decay, n evolves from the initial steady state value to the dark equilibrium ($V_{oc} = 0$) with concentration n_0. We will generally neglect the final region of decay at $V_{oc} \approx 50$ mV or less, which is poorly resolved in the current setup, hence we can assume that $n \ll n_0$. According to Equation 1, the transient is described by Equation (3):

$$\frac{dn}{dt} = -U(n) \quad (3)$$

Intuitively, the electron lifetime can be defined as Equation (4):

$$\tau_n^{-1} = -\frac{1}{n}\frac{dn}{dt} \quad (4)$$

Hence, Equation (5):

$$\tau_n = \frac{n}{U(n)} \quad (5)$$

This definition is exact only for a linear system with $U = k_r n$ (k_r = rate constant for recombination).[6] The more general and rigorous concept of the lifetime is discussed below, and we show that Equation (5) is generally justified for the decay in nonlinear dye solar cells. Using Equations (2) and (5), we can derive the lifetime from $V_{oc}(t)$ by Equation (6):

$$\tau_n = -\frac{k_B T}{e}\left(\frac{dV_{oc}}{dt}\right)^{-1} \quad (6)$$

Therefore, $\tau_n(V_{oc})$ is given by the reciprocal of the derivative of the decay curve normalised by the thermal voltage.

It has been suggested that the recombination reaction in dye solar cells (mediated by the electron acceptor I_2) is nonlinear, and of second order with respect to electron concentration,[4, 5, 7] in which case $U \propto n^2$. Let us consider the nonlinear recombination model, Equation (7):

$$U = -k_r n^\beta \quad (7)$$

where β is a constant. By Equation (5), the lifetime takes the form of Equation (8):

$$\tau_n = \frac{1}{k_r n^{\beta-1}} \quad (8)$$

Because Equation (8) implies $\log\tau_n = -(\beta-1)V_{oc}/59\,\text{mV} + \text{constant}$, it follows from the assumption in Equation (7) that for any $\beta \neq 1$ the electron lifetime varies exponentially with the Fermi level. In a first approximation, this hypothesis provides a good description of the experimental trends reported below, with $\beta \approx 1.4$.

Let us note, from Equation (8), that the effective recombination order can be obtained as Equation (9):

$$\beta = 1 + \frac{d\ln\tau_n^{-1}}{d\ln n} \quad (9)$$

In order to characterize in detail the variation of the lifetime, we take Equation (9) as a general definition of the β parameter without assuming it is constant. When we let β be an arbitrary function of the Fermi level, we are able to express any recombination mechanism in terms of this parameter (not only the second-order reaction, $\beta = 2$, which was taken as an intuitive starting point), by writing the recombination rate as in Equation (7). The β parameter is a convenient description of the lifetime-dependence on the Fermi level in dye solar cells because experimentally Equation (9) is found to be nearly constant. But the parameter β takes physical content when a specific kinetic model for recombination is formulated, so that the model implications can be compared with the measurements; this will be illustrated below with a model including trapping effects.

By substituting Equation (2) into Equation (9), we get the expression, Equation (10):

$$\beta = 1 + \frac{k_B T}{e}\frac{d\ln\tau_n^{-1}}{dV_{oc}} \quad (10)$$

An alternative way to express Equation (9) is the following Equation (11):

$$\beta = 1 + \frac{d\tau_n}{dt} \quad (11)$$

Having introduced the main ideas with an intuitive approach, we now give a rigorous definition of the lifetime. The lifetime is defined for the exponential decay following a small variation of the Fermi level, for example, from a steady state at I_0 to that at $I_0 + \Delta I_0$. Under these conditions, we can write $n = \tilde{n} + \Delta n$, where $\tilde{n}$ is the steady state value that obeys $U(\tilde{n}) = \alpha I_0$, and $\Delta n(t)$ is the small variation for the recovery towards the new steady state. Linearization of Equation (1) shows that the transient is controlled by Equation (12):

$$\frac{d(\Delta n)}{d}t = -\left(\frac{d\tilde{U}}{d\tilde{n}}\right)\Delta n \quad (12)$$

with a step impulse $\alpha\Delta I_0$ at $t = 0$. According to Equation (12), time evolution of $\Delta n(t)$ is exponential and the lifetime is given by Equation (13) at each steady state.

$$\tau_n = \left(\frac{d\tilde{U}}{d\tilde{n}}\right)^{-1} \quad (13)$$

The quantity τ_n, which corresponds to the time constant in IMVS [see Equation (31)], could be measured also in the time domain, which monitors the decay after a small step of the illumination, at different steady states. However, we now show that the measurement of the OCVD from a steady state to the dark equilibrium gives similar information while being a much faster method. When we apply the general definition in Equation (13) to Equation (7) with $\beta = \text{constant}$, we get $\tau_n^{-1} = \beta k_r n^{\beta-1}$, which is just Equation (8) except for the factor β. Therefore, when the lifetime varies exponentially with V_{oc} with β close to 1 (which is confirmed by the observations reported below), then Equation (6) is an excellent approximation. In other words, a rapid method for obtaining τ_n and β consists in applying Equations (6) and (10) to $V_{oc}(t)$, and this procedure is used below in the analysis of experimental results.

We note that Equation (6) will not be a fair approximation in the presence of large oscillations of β. In that case, the fully correct expression $\tau_n(V_{oc})$ should be used. From Equation (13), Equation (14) readily follows.

$$\tau_n^{-1} = -\frac{e}{k_B T}\frac{dV_{oc}}{dt} - \left(\frac{dV_{oc}}{dt}\right)^{-1}\frac{d^2V_{oc}}{dt^2} \quad (14)$$

Let us further verify the accuracy of Equation (6). If we denote τ_n the approximation defined in Equation (6), we can express Equation (14) as Equation (15).

$$\tau_n = \frac{\tau_n'}{1 + \frac{d\tau_n'}{dt}} \quad (15)$$

The correction to Equation (6) is contained in the denominator of Equation (15), which is just the number defined in Equation (11). Therefore, as already stated above, $\tau_n \approx \tau_n'$, provided that β is close to 1.

Our analysis developed so far underlines the decay of the carrier density n in extended states (cb). This is because, according to the current understanding [as stated in Equation (2)], these states communicate with the substrate, so that the electrons in extended states maintain the photovoltage in the outer circuit. Therefore, the decay of n is directly responsible for the OCVD. However, TiO_2 particles are known to contain a large number of traps, and the density of trapped charge may

largely outnumber that of free electron charge.[8] It must be realized that the measured lifetime τ_n does not in general correspond to the free carrier lifetime but consists of an average of characteristic times for survival of free and trapped electrons. The general formalism developed above also serves to describe this type of situation. This is because we have left open the β dependence on the free electrons Fermi level, E_{Fn}. Thus, the $U(n)$ in Equation (3) can take the meaning of an effective recombination rate for free carriers that counts also the contribution of trapping and detrapping.

To illustrate this important point, we adapt the classical model of Rose for the response-time dependence on light intensity in photoconductors[9] (a recent formulation of a similar model for dye solar cells is presented in ref. [10]). Let us consider a localized level in the band gap with total density (per unit volume) N_L and fractional occupancy f_L, so that the density of the localized electrons is $n_L = N_L f_L$. The equations of conservation for free and trapped electrons are as follows, Equations (16) and (17).

$$\frac{dn}{dt} = -\varepsilon_t n(1-f_L) + \varepsilon_d N_L f_L - U_0(n) \tag{16}$$

$$\frac{df_L}{dt} = \varepsilon_t \frac{n}{N_L}(1-f_L) - \varepsilon_d f_L \tag{17}$$

In Equation (16), ε_t and ε_d are the probabilities of trapping and release, and $U_0(n)$ is the rate of injection of cb electrons into the electrolyte acceptor species. About this last term, we take the simplest assumption, Equation (18), so that τ_{n0} is the constant free-carrier lifetime, that is, the lifetime with respect to injection to the electrolyte in the absence of trapping.

$$U_0 = -\frac{n}{\tau_{n0}} \tag{18}$$

From Equations (16) and (17), we can write Equation (19).

$$\frac{d}{dt}(n+n_L) = -U_0(n) \tag{19}$$

Linearizing, as before, for a small variation of the Fermi level ($n(t) = \tilde{n} + \Delta n(t)$), we obtain Equation (20).

$$\left(1+\frac{\partial \tilde{n}_L}{\partial \tilde{n}}\right)\frac{d\Delta n}{dt} = -\frac{d\tilde{U}_0}{d\tilde{n}}\Delta n \tag{20}$$

This last equation assumes the quasistatic condition that the free and localized electrons remain at a common equilibrium under the discharge process, $\Delta\tilde{n}_L(t) = (\partial\tilde{n}_L/\partial\tilde{n})\Delta n(t)$. It follows that the observed recombination time (τ_n), which in ref. [9] is denoted as the response time, is given by Equation (21).

$$\tau_n = \left(1+\frac{\partial \tilde{n}_L}{\partial \tilde{n}}\right)\tau_{n0} \tag{21}$$

According to Equation (21), trapping and detrapping delays the discharge of cb electrons to solution (the factor $\frac{\partial n_L}{\partial n}$ is positive), which is also the intuitive conclusion. Furthermore, the delay by trapping and detrapping is important only if the trap density is significant so that $(\partial\tilde{n}_L/\partial\tilde{n}) \gg 1$, and this will be assumed hereafter.

The formalism can be readily extended for a continuous distribution of internal traps. In this case, Equation (21) can be interpreted in the following way: To produce a small variation of the Fermi level, it is necessary to release the electrons in a slice of the traps, dn_L, near the Fermi level, to the cb, and then to release the cb electrons into the solution. For a distribution of localized states $g(E)$ (per unit volume and electronvolt), the delay factor takes approximately the form of Equation (22):[11]

$$\frac{\partial n_L}{\partial n} = \frac{k_B T}{n} g(E_{Fn}) \tag{22}$$

The exponential distribution with the tailing parameter T_c (with $\alpha = T/T_c$) is defined in Equation (23),

$$g(E) = \frac{N_L}{k_B T_c}\exp[(E-E_c)/k_B T_c] \tag{23}$$

and we obtain from Equation (22) the result, Equation (24), where N_c is the density of cb states.

$$\frac{\partial n_L}{\partial n} = \alpha \frac{N_L}{N_c^\alpha} n^{\alpha-1} \tag{24}$$

Therefore, Equation (25), where A is a constant.

$$\tau_n = A n^{\alpha-1}\tau_{n0} \tag{25}$$

Using Equation (9), we arrive at the effective recombination order for this model, Equation (26).

$$\beta = 2-\alpha \tag{26}$$

We note that the value of α, which stands for an exponential distribution of traps, usually lies between 0.4 and 0.7, as determined by transport measurements,[5, 8, 12] which means that the value of β defined by Equation (10) is 1.3 – 1.6. Thus, for the model of Equation (25), the simplification indicated according to Equation (15) (requiring that β is close to 1) can be maintained. Note that Equation (26) corresponds to linear recombination of free electrons [Eq. (18)] and does not contain the second-order reaction mechanism. We remark also that the effect of internal traps on the lifetime applies as well if cb electrons are captured preferentially by the oxidised dye, so that Equation (26) describes this case as well.

The results of our measurements and the application of the procedures of analysis outlined above are presented in Figure 1. The data shown in Figure 1a consist of four OCVD decay curves starting at different initial steady states at progressively lower light intensities. For a linear system with a unique τ_n, the $V_{oc}(t)$ characteristic would decay linearly with time. The curves indicate a supralinear decay where the lifetime recedes to larger values when E_{Fn} progressively separates from the cb. In fact, Figure 1b shows the lifetime values obtained from Figure 1a using Equation (6). The lifetime dependence on V_{oc} is exponential in broad terms, spanning three decades from 20 ms to 20 s when V_{oc} decreases starting at $\approx$0.6 V.

The comparison of decay curves from the different initial states in Figure 1b shows that the evolution of the lifetime is very similar starting at different points, $V_{oc} \approx 0.7$, 0.6, or 0.5 V. This

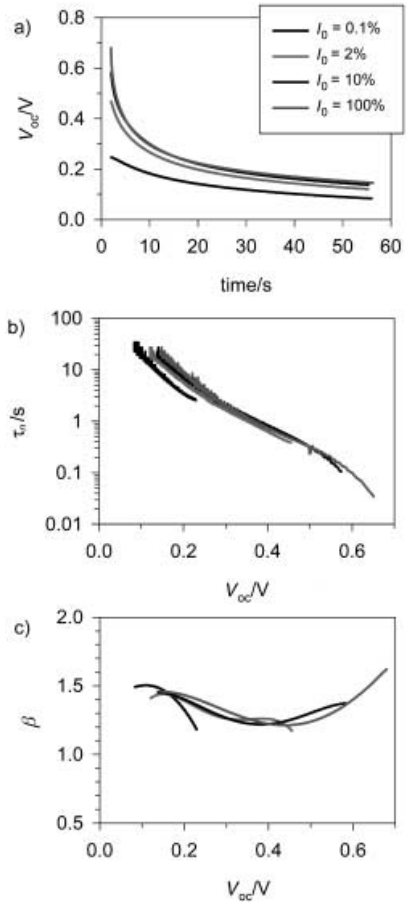

Figure 1. *Experimental V_{oc} decay results of a single titania dye solar cell starting at four different initial steady states, as indicated by the relative light intensities incident in the solar cell. The arrows indicate the starting open-circuit voltage in each decay. a) Measured $V_{oc}(t)$. b) The electron lifetime derived from Equation (6) as a function of V_{oc}. c) Recombination β-parameter (effective recombination order) derived from Equation (10) as a function of V_{oc}.*

result shows that the evolution proceeds without memory of the preceding states, which confirms the contention that the OCVD corresponds to a succession of steady states. In the measurement that begins at the lowest V_{oc} ($\approx$0.3 V), the lifetime shows a similar trend as in the others at consistently lower values by a factor of five. We suspect that this difference is related to extremely slow kinetics of deep-surface states (recombination centers), but further work is required to clarify this effect.

By using Equation (10), we find the parameter β, which is presented in Figure 1 c. In essence, this β parameter is a suitable normalization of the local slope of Figure 1 b ($\beta = 1$ when τ_n is a constant). The β parameter shows a nearly constant value of 1.3 at medium V_{oc} and increases to 1.5 both at higher and lower photopotentials. Therefore, the model of discharge mediated by trapping and detrapping summarised in Equation (26) with a tailing parameter $\alpha \approx 0.5$ provides a good overall explanation of the measurements reported in Figure 1. However, we have presented this model as a basic illustration of the effects of trapping on the observed decay times. Other options to consider include, for instance, recombination through surface states, which extends Equation (17) by an electron-transfer term, and also a possible distribution of surface states as indicated in ref. [2]. As an example of a more general model, we may consider that the free carrier lifetime is given by an expression of the type $\tau_{n0}^{-1} = k_r n^{\beta_0 - 1}$ (Equation (8)). Then, by the same arguments leading to Equation (26), we obtain Equation (27).

$$\beta = (1 - \alpha) + \beta_0 \tag{27}$$

This equation shows that, in general, the effective recombination order contains contributions both from trapping, detrapping and charge-transfer mechanisms (for instance for second-order recombination, $\beta_0 = 2$, and trapping, we obtain $\beta = 3 - \alpha$ Therefore, in order to explain in detail the observed $\beta(V_{oc})$ (including the clear oscillations observed in Figure 1), a number of models should be compared,[2–5, 7, 8, 13] and this is left as a matter for further investigation.

As mentioned, the IMVS response is measured at open circuit at a given steady state, so that the relaxation time that is recorded is the electron lifetime of that particular steady state. Next, we compare the full correspondence of the OCVD and IMVS methods.

The IMVS operates by measuring the time-modulated component ΔV_{oc} in $\bar{V}_{oc} + \Delta V_{oc} \exp(i\omega t)$ with respect to a small periodic perturbation (ΔI_0) of the illumination $\bar{I}_0 + \Delta I_0 \exp(i\omega t)$. According to Equation (1), the free electron density will oscillate with an amplitude determined by Equation (28).

$$\frac{d(\Delta n\, e^{i\omega t})}{dt} = -\frac{d\tilde{U}}{d\tilde{n}}\, \Delta n\, e^{i\omega t} + \alpha_{abs} \Delta I_0\, e^{i\omega t} \tag{28}$$

Hence, Equation (29), where τ_n is the same as in Equation (13).

$$\Delta n = \frac{\alpha_{abs} \Delta I_0}{i\omega + 1/\tau_n} \tag{29}$$

Linearizing Equation (2), we obtain Equation (30).

$$\Delta n = \frac{\tilde{n}e}{k_B T} \Delta V_{oc} \tag{30}$$

In conclusion, Equation (31):

$$\frac{\Delta V_{oc}}{\Delta I_0} = \frac{\alpha k_B T}{ne} \frac{1}{i\omega + 1/\tau_n} \tag{31}$$

Therefore, on the assumption $U(n)$, the IMVS response is represented by an arc in the complex plane, and the characteristic angular frequency is the inverse of the lifetime in Equation (13), which shows the agreement of the results of the two methods.

Figure 2 shows that in fact the electron lifetime, τ_n, obtained from the time-domain large perturbation method of OCVD is in fact in excellent accordance with the small signal frequency domain technique (IMVS) results reported in the literature. The match of τ_n results shown in Figure 2 is highly significant because it shows a convergence of independent techniques. We note however that being a continuous measurement the OCVD provides information at very high voltage resolution, thus being more informative than IMVS in this respect.

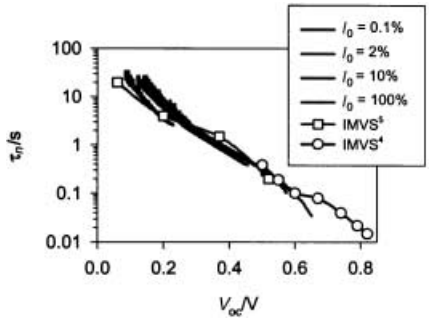

Figure 2. *The electron lifetime as a function of V_{oc} in different titania dye solar cells with the redox couple I^-/I_3^-. The lines correspond to decay results starting at four different initial steady states (same data as Figure 1b). Circles correspond to IMVS results reported in ref. [5] (by combining the data $\tau_n(I_0)$ and $V_{oc}(I_0)$ given separately in this reference) and in ref.[4] (data from Figure 10a, TBP, which appears to be the closest configuration to our own solar cell).*

In summary, we have shown that the analysis of the decay of photovoltage at open-circuit conditions in dye solar cells constitutes a very simple procedure for obtaining the relevant information on the electron lifetime τ_n and also the parameter β (effective recombination order) that governs the change of the lifetime. It was found that the lifetime dependence on V_{oc} is exponential in broad terms, spanning three decades from 20 ms to 20 s, when V_{oc} decreases by about 0.6 V, which is in agreement with previously reported values obtained by IMVS. In contrast, the parameter β with an average value of 1.4 and a residual variation with the photopotential suggests a more detailed picture in comparison with IMVS. This parameter demonstrates the power of the OCVD technique with respect to the voltage resolution.

Experimental Section

All chemicals were purchased (Aldrich Chemical Co.) and used as received. Nanosize TiO_2 suspensions were synthesised using titanium tetraisopropoxide precursor as previously reported.[14] In brief, the titanium tetraisopropoxide dissolved at 1:1 ratio in isopropanol was hydrolysed by acetic acid (pH 2) under rigorous stirring. After overnight aging, the isopropanol was evaporated at 82 °C, and the suspension was autoclaved at 250 °C for 13 h, which resulted in 20-nm crystals.

Conducting glass substrate (8 Ω/square F-doped SnO_2, Libby Owens Ford), was cleaned with soap, rinsed with deionised water (18.2 MΩ), and dried in an air stream. The TiO_2 suspension was spread on the conducting substrate by using a glass rod, using adhesive tapes as spacers. After the films were dried under ambient conditions, they were sintered in air at 450 °C for 30 min.[14] The TiO_2 film thickness measured with a profilometer (Mitutoyo, Sueftest SV 500) was 3 μm.

The electrodes were sensitised by using the N3 dye *cis*-di(isothiocyanato)-bis(4,4-dicarboxy-2,2-bipyridine) ruthenium(II) (Solaronic SA). For dye adsorption, the electrodes were immersed overnight in a 0.5 mM solution of dye in absolute ethanol. To avoid water, the films were heated to 120 °C before immersion in the dye solution.

A sandwich-type configuration was employed to measure the performance of the dye-sensitised solar cell using an F-doped SnO_2 film coated with Pt as a counter electrode.[15] The electrolyte solution consisted of 0.5 M *tert*-butylammonium iodine (TBAI), 0.05 M I_2, and 2.7 mM 4-*tert*-butylpyridine (TBP) in 1:1 acetonitrile-3-methyl-2-oxazolidinone (NMO). Illumination of the cell was done with a 150-W Xe lamp calibrated to 1 sun.

For the decay measurements, the cell was illuminated to a steady voltage. The illumination was turned off with a shutter. Placing neutral density filters in the illumination path performed a systematic change of initial steady-state conditions. The OCVD was recorded by an Ecochemie potentiostat equipped with a short-interval sampling module. Typically, the measurement interval was 10 – 50 ms. The decay analysis refers only to values measured after the shutter obtained full darkness.

J.B. acknowledges the support of this work by the Fundació Caixa Castelló, project P1B99-04. A.Z. acknowledges the support of this work by the Israeli Ministry of Science.

[1] B. O'Regan, M. Grätzel, *Nature* **1991**, *353*, 737.
[2] J. Bisquert, A. Zaban, P. Salvador, *J. Phys. Chem. B* **2002**, *106*, 8774.
[3] I. Montanari, J. Nelson, J. R. Durrant, *J. Phys. Chem. B* **2002**, *106*, 12203.
[4] G. Schlichthörl, S. Y. Huang, J. Sprague, A. J. Frank, *J. Phys. Chem. B* **1997**, *101*, 8141.
[5] A. C. Fisher, L. M. Peter, E. A. Ponomarev, A. B. Walker, K. G. U. Wijayantha, *J. Phys. Chem. B* **2000**, *104*, 949.
[6] S. Södergren, A. Hagfeldt, J. Olsson, S. E. Lindquist, *J. Phys. Chem.* **1994**, *98*, 5552.
[7] N. W. Duffy, L. M. Peter, R. M. G. Rajapakse, K. G. U. Wijayantha, *J. Phys. Chem. B* **2000**, *104*, 8916.
[8] J. Nelson, *Phys. Rev. B* **1999**, *59*, 15374.
[9] A. Rose, *Concepts in Photoconductivity and Allied Problems*, Interscience, New York, **1963**.
[10] A. V. Barzykin, M. Tachiya, *J. Phys. Chem. B* **2002**, *106*, 4356.
[11] F. Fabregat-Santiago, I. Mora-Seró, G. Garcia-Belmonte, J. Bisquert, *J. Phys. Chem. B* **2003**, *107*, 758.
[12] R. Könenkamp, *Phys. Rev. B* **2000**, *61*, 11057.
[13] S. Y. Huang, G. Schlichthörl, A. J. Nozik, M. Grätzel, A. J. Frank, *J. Phys. Chem. B* **1997**, *101*, 2576.
[14] A. Zaban, S. T. Aruna, S. Tirosh, B. A. Gregg, Y. Mastai, *J. Phys. Chem. B* **2000**, *104*, 4130.
[15] A. Zaban, S. G. Chen, S. Chappel, B. A. Gregg, *Chem. Commun.* **2000**, *22*, 2231.

Received: December 12, 2002 [Z615]
Revised: May 22, 2003